

n - p Differential Cross Section and Polarization at 199 MeV*A. R. THOMAS,[†] D. SPALDING,[‡] AND E. H. THORNDIKE*Department of Physics and Astronomy, University of Rochester, Rochester, New York*

(Received 25 September 1967)

The relative differential cross sections and polarization parameters for free n - p scattering, and for the reaction $n+d \rightarrow p+2n$ in which only the proton is detected (bound n - p scattering), have been measured at an incident energy of 199 MeV, at two-nucleon c.m. angles between 77° and 158° . The neutron beam used, created by charge-exchange scattering of a polarized proton beam on a deuterium target, had an energy spread of ± 12 MeV, a polarization of 73%, and an intensity of 1000 n /sec. The beam polarization was determined by comparing the asymmetry measured in the reaction $n+d \rightarrow p+2n$ with the polarization of the (previously studied) charge-symmetric reaction $p+d \rightarrow n+2p$, in which only the neutron is detected. The differential cross section σ and the polarization P , for free n - p scattering, the ratio R_M of the bound to the free cross section, and the difference $P-P_b$ between the free and bound polarization parameters are listed.

$\theta_{c.m.}$ (deg)	σ	P	R_M	$P-P_b$
158.1	1.000 ± 0.021	-0.071 ± 0.012	0.665 ± 0.044	$+0.027 \pm 0.018$
148.1	0.836 ± 0.017	-0.117 ± 0.011	0.648 ± 0.043	-0.003 ± 0.019
137.8	0.701 ± 0.015	-0.125 ± 0.009	0.675 ± 0.044	-0.003 ± 0.015
127.4	0.578 ± 0.013	-0.125 ± 0.010	0.660 ± 0.044	$+0.019 \pm 0.018$
117.1	0.461 ± 0.010	-0.111 ± 0.011
96.3	0.320 ± 0.008	-0.075 ± 0.014	0.630 ± 0.044	-0.035 ± 0.026
86.6	0.292 ± 0.007	0.029 ± 0.017
76.9	0.273 ± 0.008	0.132 ± 0.028	0.597 ± 0.043	0.071 ± 0.041

A 10% systematic error in P , due to uncertainty in beam polarization, is *not* included in the listed error. The cross-section measurements agree with those of Kazarinov and Simonov and with the phase-shift solution (Y-IV) _{n,p} of Breit *et al.* but disagree with the older measurements of Guernsey, Mott, and Nelson. The polarization measurements are in satisfactory agreement with the (less accurate) results of Tinlot and Warner, but in only fair agreement with the phase-shift solution (Y-IV) _{n,p} . The ratio R_M , typically 0.65 ± 0.04 , is significantly smaller than that given by an impulse-approximation calculation, typically 0.76. The difference between polarization parameters for free and bound scattering is consistent with an impulse-approximation calculation but also consistent with zero.

I. INTRODUCTION

A STUDY of the n - p interaction near 200 MeV has been in progress at Rochester for several years. Measurements of the triple-scattering parameters^{1,2} R_t and D_t , and of n - p bremsstrahlung³ have been previously reported. Here we present measurements of the differential cross section and polarization in n - p elastic scattering, at eight center-of-mass (c.m.) angles between 77° and 158° . In addition to the scattering of neutrons by free protons, some measurements were made for the scattering of neutrons by protons bound in deuterium.

A novel feature of the present experiment is the neutron beam used. It is created from a polarized proton beam by a charge-exchange scattering on deuterium. It

is characterized by a high polarization (73%), good energy definition (± 12 MeV), and very low intensity (1000 n /sec). The method of determining the beam polarization, also novel, is based on the equality of the asymmetry parameters for the charge-symmetric reactions $n+d \rightarrow p+2n$ and $p+d \rightarrow n+2p$. The preparation of the neutron beam and the determination of its characteristics are discussed in Sec. II.

The cross-section and polarization measurements proper are quite conventional. The neutron beam impinges upon a liquid-hydrogen target, and recoil protons are detected with scintillation counter telescopes. (For measurements with protons bound in deuterium, the hydrogen target is replaced with a deuterium target.) These experimental procedures are discussed in Sec. III. Corrections and errors are discussed and results presented in Sec. IV.

A recent review⁴ of experiments bearing on the nucleon-nucleon interaction near 210 MeV deferred a discussion of n - p differential cross section. This discussion and one of the n - p polarization is given in Sec. V. Also given are a comparison of the results for free protons with the predictions of recent phase-shift analyses, and a comparison of the results for bound protons with an impulse-approximation calculation.

* Work supported by the U. S. Atomic Energy Commission. This work is based on a thesis submitted by A. R. Thomas in partial fulfillment of the requirements for the Ph.D. degree in Physics at the University of Rochester, Rochester, New York.

[†] Present address: Analytic Services, Inc., Falls Church, Va.

[‡] Present address: Sarah Mellon Scaife Radiation Laboratory, University of Pittsburgh, Pittsburgh, Pa.

¹ N. W. Reay, E. H. Thorndike, D. Spalding, and A. R. Thomas, Phys. Rev. **150**, 801 (1966).

² D. Spalding, A. R. Thomas, and E. H. Thorndike, Phys. Rev. **158**, 1338 (1967).

³ P. F. M. Koehler, K. W. Rothe, E. H. Thorndike, Phys. Rev. Letters **18**, 933 (1967); P. F. M. Koehler, K. W. Rothe, E. H. Thorndike, Phys. Rev. (to be published).

⁴ E. H. Thorndike, Rev. Mod. Phys. **39**, 513 (1967).

This experiment is described in greater detail elsewhere.⁵

II. NEUTRON BEAM

A. Principles

The problem of making a polarized neutron beam from an unpolarized proton beam is usually solved by a one-step process; a target (e.g., beryllium) is bombarded with unpolarized protons, and the neutrons emerging at some nonzero angle (e.g., 30°) are defined into a beam. This method gives low beam polarization ($\lesssim 20\%$), and poor energy definition. By using time-of-flight methods in conjunction with the above approach, Bowen *et al.*⁶ achieved good energy definition, but still had low beam polarization.

Hobbie and Miller⁷ first used a two-step process to make a polarized neutron beam. They produced (unpolarized) neutrons at 0° by bombarding beryllium with unpolarized protons. The neutrons so produced were polarized by scattering from a second (carbon) target. A polarization of 43% was achieved. Beam intensity was low, and energy definition was very poor.

We have also used a two-step process, but have reversed the order. A proton beam is first polarized by scattering from carbon at 15° . The protons are then converted to neutrons by the charge-exchange scattering on deuterium, $p+d \rightarrow n+2p$. The scattering angle can be chosen so that most of the polarization is transferred from the proton to the neutron, and so that the energy definition of the neutrons is good. Specifically, charge-exchange scattering is selected at a lab angle of 10° , in the plane containing the incident-proton polarization. In this geometry, transfer of polarization is governed by the triple-scattering parameter $R_t(10^\circ)$ which has a value¹ of -0.84 ; that is, the neutron polarization is -0.84 times the incident-proton polarization.

The charge-exchange reaction on deuterium at small angles is relatively monoenergetic because of the strong s -wave final-state interaction of the two protons. Measday⁸ charge-exchange scattered a proton beam from deuterium at 0° to make a very monoenergetic (but unpolarized) neutron beam. As the angle increases from zero, the energy spread increases. An impulse-approximation calculation indicates that at 10° , 80% of the neutrons lie in a 10-MeV-wide interval, still relatively monoenergetic.

The neutron beam which we have achieved in this way is characterized by a high polarization (73%), good energy definition (± 12 MeV), and very low intensity (1000 n /sec). The sacrifice of intensity to achieve high polarization and good energy definition produced a beam of so low intensity as to be of limited use. How-

ever, the same approach, starting with a higher-intensity proton beam such as would be available at a "meson factory," would produce a very useful beam.

B. Beam Layout

Plan and elevation views of the neutron-beam layout are shown in Fig. 1. The 212-MeV, 85% polarized proton beam of the University of Rochester 130-in. synchrocyclotron emerges from a bending magnet (H), is monitored by an air ion chamber (IC), passes through a 5-in.-diam liquid-deuterium target (DI), and buries itself in the steel yoke of a magnet. The spin-flip magnet (SFM), embedded in a steel and concrete shielding wall, offers a $2\frac{3}{4}$ -in.-wide by 5-in.-high aperture to neutrons emerging from the target at 10° in the vertical plane. This plane contains the polarization vector of the incident proton beam $\langle \sigma_p \rangle$. When the magnet is off, the neutron beam collimated by the magnet has its polarization $\langle \sigma_n^{off} \rangle$ in the direction shown. With the magnet turned on and appropriately adjusted, the neutron spins precess through 180° about the field lines, which are normal to the vertical plane. Hence the neutron-beam polarization changes sign. With the magnet off, about 1–2 times as many protons as neutrons pass through it. These protons are eliminated by an anticoincidence counter ($\bar{1}$) at the magnet exit. With the magnet on, the protons are swept out of the beam.

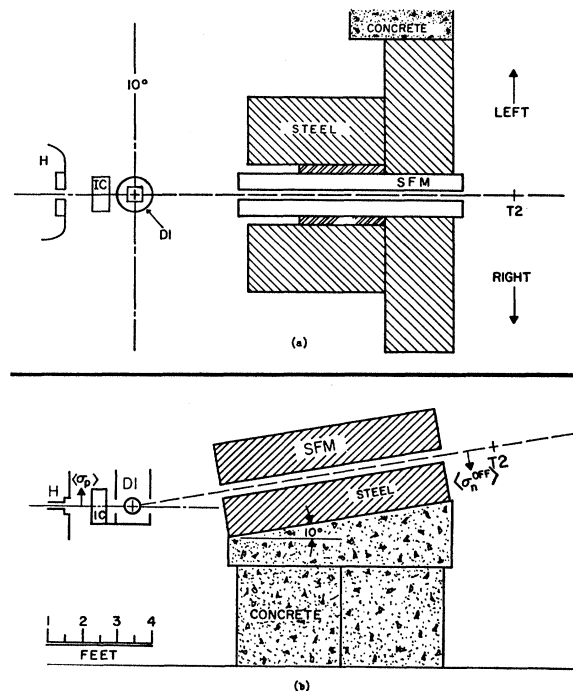


FIG. 1. Plan and elevation views of the neutron beam layout. The line labeled 10° in the plan view divides the figure into two parts: that to the left is the true horizontal plane, while that to the right is tilted at 10° to the horizontal. T2 marks the position of the hydrogen target. Other symbols are defined in the text.

⁵ A. R. Thomas, Ph.D. thesis, University of Rochester, 1967 (unpublished).

⁶ P. H. Bowen, G. C. Cox, G. B. Huxtable, A. Langsford, J. P. Scanlon, and J. L. Thresher, *Phys. Rev. Letters* **7**, 248 (1961).

⁷ R. K. Hobbie and D. Miller, *Phys. Rev.* **120**, 2201 (1960).

⁸ D. F. Measday, *Nucl. Instr. Methods* **40**, 213 (1966).

C. Energy Spectrum

The neutron-beam energy spectrum has been obtained both by measurement and by calculation. The measurement was performed by letting the beam impinge upon a liquid-hydrogen target, and taking a range curve of the protons recoiling at 15° . Effects due to the finite size of the hydrogen target and of the recoil proton telescope were unfolded to give the energy spectrum of the neutron beam, shown in Fig. 2. The range-energy tables of Rich and Madey⁹ were used to obtain the final neutron-energy spectrum.

The calculation began with an impulse-approximation calculation of the neutron-energy spectrum from the reaction $p+d \rightarrow n+2p$, initiated by monoenergetic protons. This spectrum was then "folded" with the measured energy spectrum of the primary proton beam and the finite thickness of the liquid deuterium target, to give the neutron-beam-energy spectrum.

Calculation and measurement are in good agreement. The calculated mean energy is 199.6 ± 2.0 MeV, while the measured mean energy is 199.0 ± 1.5 MeV. The calculated and measured rms widths are 11.2 and 11.8 MeV, respectively. The main contribution to the width of the neutron spectrum was the width of the primary proton spectrum; a monoenergetic proton beam would have yielded a neutron beam with a width half as large.

D. Beam Polarization

Beam polarizations are measured by scattering the beam from some target, in a reaction whose asymmetry parameter can be independently determined. The beam polarization is then the ratio of the measured asymmetry to the asymmetry parameter; the standard reaction is small-angle elastic scattering from a high- Z nucleus. The interference between nuclear scattering and the Coulomb scattering of the neutron magnetic moment gives a large and calculable asymmetry parameter.

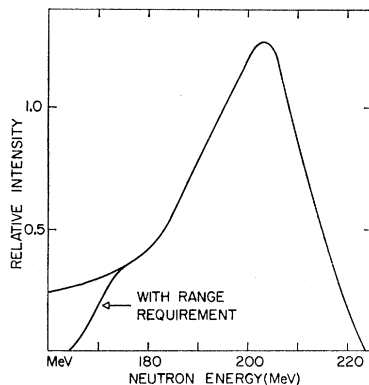


Fig. 2. The energy spectrum of the neutron beam as measured, and as modified by the range requirement used in the telescopes at a lab angle of 15° . Other lab angles give similar results.

⁹ M. Rich and R. Madey, University of California Radiation Laboratory Report No. UCRL-2301 (unpublished).

Unfortunately, the large size, appreciable angular divergence, and low intensity (as compared to room background) of our neutron beam preclude this approach.

Instead, we have used the reaction $n+d \rightarrow p+2n$. The asymmetry parameter of the *charge-symmetric* reaction $p+d \rightarrow n+2p$ has been measured at the appropriate energy and over a useful range of angles.¹⁰ To the extent that charge symmetry is valid, the asymmetry parameters for the two reactions should be equal. The only anticipated breaking of charge symmetry, that

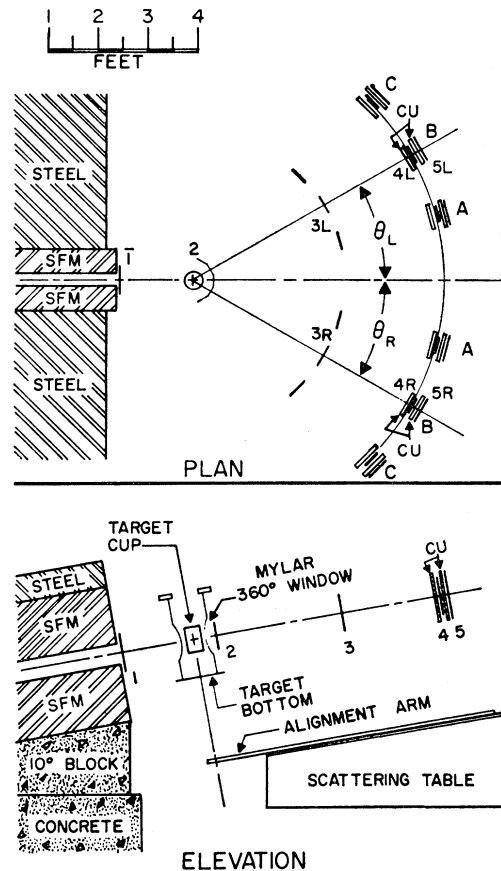


Fig. 3. Plan and elevation views of the layout for the polarization and cross-section measurements.

due to Coulomb effects, has a negligible effect on the symmetry parameter at moderate scattering angles.

In addition to determining the beam polarization, a study of the reaction $n+d \rightarrow p+2n$ is interesting in its own right. It is effectively $n-p$ scattering from a proton bound in deuterium, and can be discussed within the framework of the impulse approximation. The experimental procedure is treated in Sec. III, and the data are analyzed in Sec. IV, to give a beam polarization of 0.73 ± 0.08 .

¹⁰ D. Spalding, A. R. Thomas, N. W. Reay, and E. H. Thorndike, Phys. Rev. **150**, 806 (1966).

III. EXPERIMENTAL APPARATUS AND PROCEDURES

Plan and elevation views of the layout for the polarization and cross-section measurements proper are shown in Fig. 3. The neutron beam emerges from the SFM, passes through an anticoincidence counter (1), and strikes a target of liquid hydrogen. Recoil protons pass through a scintillation counter (2), and then through any one of six scintillation counter telescopes (345). Copper absorbers between 3 and 4, and between 4 and 5, are chosen to set a threshold of 169 MeV on the incident neutron energy. The telescopes are arranged in three pairs, each with its members at equal angles on opposite sides of the beam. Data are taken both with the spin-flip magnet on and off. The sum of the counting rates is a measure of the cross section; the asymmetry in the counting rates is a measure of the polarization.

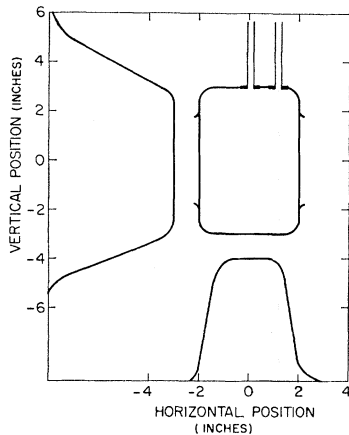


Fig. 4. Neutron beam intensity profiles at the hydrogen-target position (T2). The positions of the target cup and fill pipes are indicated.

Use of a spin-flip magnet and a pair of counters, simultaneously to the left and right of the beam, eliminates many sources of spurious asymmetries.

The liquid-hydrogen target cup was an all Mylar cylinder, 6 in. high by 4 in. in diam, suspended from two $\frac{1}{4}$ -in.-diam thin-walled stainless-steel pipes. The cylinder side and bottom were 0.005 in. thick, the top 0.010 in. thick. The target vacuum chamber had a 360° window of 0.010-in. Mylar, thus minimizing background by keeping material out of the beam. The window was 10 in. high, 8 in. in diam at its ends, and bowed in to a 5 in. diam at its center. The shape of the beam at the target cup is shown in Fig. 4. Note that the vertical collimation, provided by the coils of the spin-flip magnet, is less sharp than the horizontal collimation, provided by the yoke.

Counter 2 restricted the view of the recoil-proton telescopes to the immediate area of the target; without this counter, background and random-coincidence rates were excessively high. Because counter 2 was in the neutron beam, it contributed background counts. This

TABLE I. Counter sizes in 345 telescopes A, B, and C, and the angles at which each telescope was used. Dimensions are width \times height \times thickness, in inches.

	A (10°,15°,20°)	B (20°,25°,30°)	C (40°,45°,50°)
3	$4\frac{1}{2} \times 10 \times \frac{1}{4}$	$5 \times 15 \times \frac{1}{4}$	$5 \times 13\frac{1}{2} \times \frac{1}{4}$
4	$4 \times 10 \times \frac{1}{4}$	$5 \times 18 \times \frac{1}{4}$	$5 \times 24 \times \frac{1}{8}$
5	$5\frac{1}{2} \times 12 \times \frac{1}{4}$	$6 \times 20 \times \frac{1}{4}$	$6 \times 26 \times \frac{1}{8}$

background was minimized by constructing the counter from three $\frac{1}{16}$ -in.-thick counters, C2, L2, and R2. C2 was 3 in. wide by 7 in. high, and aligned symmetrically on the beam line; most of the nonscattered beam particles traversed this counter. Placed on each side of C2 with a slight overlap, and covering the rest of the angular region, were counters R2 and L2, each consisting of two pieces of scintillator $3\frac{1}{4}$ in. wide by 7 in. high, glued together with an enclosed angle of 150°. For recoil proton angles greater than 30°, only one counter, either R2 or L2, was needed, and hence the counter-associated background coming from C2 was eliminated. For angles less than or equal to 30°, the signals from C2 were combined with the signals from R2 or L2.

The dimensions of the three pairs (A,B,C) of recoil proton telescopes (345) and the angles at which each was used, are given in Table I. Counter 4, which was the defining counter, was 60 in. from the target. Note that the counter heights increase as the recoil proton angle increases, as can be done without worsening the definition of the azimuthal angle ϕ .

The fast logic with the 22 counters was performed with Chronetics Series 100 modules.

To take data with "protons bound in deuterium," the only change was to modify the target so that it could be filled with liquid deuterium rather than liquid hydrogen. The cup and outer window were not changed, nor was any other aspect of the apparatus or procedures. Unfortunately, technical difficulties were experienced with the target, and it was not always full of liquid deuterium, but rather had a content that varied with time. This introduced no errors into the polarization measurement, but introduced large errors into the cross-section measurement.

In addition to the $\bar{1}2345$ coincidence rate, the delayed-coincidence rates $\bar{1}2:345$, $\bar{1}23:45$, and $\bar{1}234:5$ were periodically measured. (Our notation indicates that signals from the counters following the colon were delayed with respect to the counters preceding the colon by 52.5 nsec, the period of the rf structure of the beam.) These delayed-coincidence rates were a measure of the random coincidences. Data were taken with the target full of hydrogen, full of deuterium, and empty.

IV. ANALYSIS AND RESULTS

A. Data Reduction

Since data were collected simultaneously at three angles, a period of data collection is designated by an

TABLE II. Data-collection sequence and consistency check. For each data period the angles of A, B, and C telescopes, and the target condition are given. Also given are the number of sets with deviations δ from their means of less than one, one to two, and more than two, standard deviations (σ). The sum of these numbers is compared with a normal distribution (N.D.).

Data period	Angles	Target	Number of sets			Total No.
			$\delta \leq \sigma$	$\sigma < \delta \leq 2\sigma$	$\delta > 2\sigma$	
1	(15,25,40)	Empty	4	3	2	9
2	(15,25,40)	H ₂	13	2	0	15
3	(10,20,50)	H ₂	15	9	0	24
4	(10,20,50)	Empty	23	12	1	36
5	(20,30,45)	Empty	26	13	3	42
6	(20,30,45)	H ₂	10	4	1	15
7	(15,25,40)	H ₂	43	16	4	63
8	(15,25,40)	Empty	16	4	1	21
9	(15,25,40)	Empty				
10	(15,25,40)	D ₂				
11	(10,20,50)	D ₂				
12	(10,20,50)	Empty				
			150	63	12	225
			=66.7%	28.0%	5.3%	
			N.D.=68.3%	27.2%	4.5%	

ordered triplet (A,B,C), where A is the angle of the A telescope, etc. Periods of data collection were composed of several "sets"; each contained eight 25-min runs, alternately with the spin-flip magnet on and off, plus some shorter runs for measuring random coincidences. The time sequence of the data periods is shown in Table II. Internal consistency of a data period was checked by comparing the $\bar{I}2345$ rate (summed over all counters and magnet conditions) for each set with the average for the data period. For the hydrogen data the distribution of these deviations is shown in Table II. Only one piece of data out of 225 differs by more than three standard deviations from the mean. The distribu-

tion agrees well with a normal distribution. The deuterium data could not be analyzed this way since the amount of deuterium in the target cup varied with time.

The magnitudes of the target-empty background and of the various random coincidences are given in Table III. The only alarming random rate is the $\bar{I}23:45$ rate for 50° hydrogen, which was high because of a large 45 rate. For 50° deuterium data, absorber which had been between counters 3 and 4 was placed between counters 4 and 5, significantly reducing the 45 rate, and hence the $\bar{I}23:45$ rate. The increase of the *percentage* target-empty background for deuterium, as compared to hydrogen, was due to the lower *true* rate from deuterium; the actual background was the same in both cases.

The four rates N_{ij} (where $i=R$ or L , denotes right or left counter, and $j=on$ or off , denotes the spin-flip magnet condition) were corrected for background and randoms, and then used to calculate the quantities

$$\Sigma = N_{R-off} + N_{L-on} + N_{R-on} + N_{L-off}$$

and

$$\epsilon = (N_{R-off} + N_{L-on} - N_{R-on} - N_{L-off}) / \Sigma.$$

Σ and ϵ , after appropriate corrections, give the cross section and polarization, respectively.

B. Corrections and Errors

1. Absorber Corrections

Multiple-Coulomb or wide-angle elastic scattering of the recoil protons in the hydrogen target, counters, or absorbers cause negligible loss of counts. Inelastic scattering in the counters and absorbers, however, causes significant losses, and a correction must be applied to Σ . This "nuclear-absorption" correction was

TABLE III. Magnitude of target-empty and random rates. All ratios are compared with the background-and-random-corrected target-full rate, and are expressed as percentages.

Data period	Angle	Target	Target full			$\bar{I}2345$	Target empty		
			$\bar{I}2:345$	$\bar{I}23:45$	$\bar{I}234:5$		$\bar{I}2:345$	$\bar{I}23:45$	$\bar{I}234:5$
(1,2)	15°	H ₂	0.2%	0.1%	0.5%	15.0%	0.2%	0.2%	0.6%
	25°		0.7	0.4	0.6	16.2	0.3	0.3	0.4
	40°		0.2	1.4	0.6	7.9	1.1	3.1	0.2
(3,4)	10°	H ₂	0.3%	0.1%	0.6%	13.7%	0.0%	0.2%	0.4%
	20°		1.3	0.4	0.6	15.6	0.3	0.4	0.3
	50°		1.8	9.7	1.9	17.5	1.1	9.6	1.7
(5,6)	20°	H ₂	0.4%	0.0%	0.2%	13.8%	0.0%	0.2%	0.2%
	30°		0.6	0.5	0.3	13.1	0.5	0.7	0.4
	45°		0.8	1.4	0.2	12.8	0.9	1.4	0.5
(7,8)	15°	H ₂	0.2%	0.0%	0.2%	12.3%	0.0%	0.0%	0.0%
	25°		0.3	0.2	0.2	13.3	0.3	0.5	0.3
	40°		0.3	0.5	0.1	10.6	0.2	0.2	0.1
(9,10)	15°	D ₂	0.1%	0.1%	0.3%	21.4%	0.0%	0.2%	0.1%
	25°		0.5	0.3	0.2	23.8	0.2	0.6	0.2
	40°		0.6	0.1	0.3	19.2	0.0	2.1	0.1
(11,12)	10°	D ₂	0.1%	0.1%	0.4%	17.4%	0.0%	0.0%	0.2%
	20°		0.8	0.4	0.3	19.1	0.2	0.3	0.1
	50°		1.6	1.3	0.5	27.1	1.2	1.3	0.3

calculated from *p*-nucleus total inelastic cross sections under the assumption that any proton that experienced an inelastic event was lost. Consideration of the validity of this assumption, and of the errors on the total inelastic cross sections, suggests that the calculated loss of protons is accurate to $\pm 10\%$ of itself.

The nuclear-absorption correction factors are listed in Table IV. Properly speaking, there are two types of errors to the correction factors: a random error, estimated at $\pm 0.5\%$ of the correction factor, affecting each angle independently; and a systematic error, estimated at $\pm 10\%$ of the difference between 1.0 and the correction factor, affecting all angles together. For most purposes, however, one can ignore the systematic nature of this second error. We do so and include a random error of $\pm 0.9\%$ of the correction factor, as listed in Table V.

It should be stressed that while this correction and its error is important to the cross section, it in no way affects the polarization parameter.

2. Monitor Drift

Between data periods 2 and 7, the ion chamber monitor experienced a net drift of $(-9.2 \pm 0.8)\%$, as indicated by the change in the measured summed rates in telescopes A, B, and C. A correction must be applied to Σ for this drift.

One expects the monitor to change in one of three possible ways: a discrete change, random short-term fluctuations, or a smooth long-term change. The good internal consistency of all data periods demonstrates that the short-term fluctuations were small. Close inspection of the individual data periods does not reveal any large discrete changes. However, in all hydrogen-full data periods (2, 3, 6, and 7), the summed rates for the second half of the data period are smaller than those for the first half, implying a smooth negative drift. The four changes for data periods 2, 3, 6, and 7 are $(-0.98 \pm 0.92)\%$, $(-1.38 \pm 0.94)\%$, $(-1.40 \pm 0.64)\%$, and $(-0.92 \pm 0.78)\%$, respectively. An additional piece of

TABLE IV. Corrections to Σ due to nuclear absorption (1), monitor drift (2), solid angle (4), finite height of counter 2 (9), and variation in energy threshold with angle (12).

Angle	Data period	1 (abs)	2 (mon)	4 (Ω)	9 (ctr 2)	12 (thr)
A-15°	1, 2	0.988	0.956	1.000	1.000	1.000
B-25°		0.949	0.956	0.448	1.004	1.002
C-40°		0.892	0.956	0.339	1.009	1.036
A-10°	3, 4	1.000	0.975	1.000	1.000	0.996
B-20°		0.968	0.975	0.448	1.004	0.998
C-50°		0.862	0.975	0.339	1.009	1.075
A-20°	5, 6	0.968	1.020	1.000	1.000	0.995
B-30°		0.929	1.020	0.448	1.004	1.005
C-45°		0.875	1.020	0.339	1.009	1.056
A-15°	7, 8	0.988	1.048	1.000	1.000	1.000
B-25°		0.949	1.048	0.448	1.004	1.002
C-40°		0.892	1.048	0.339	1.009	1.036

data is the ratio of the A telescopes during period 6 (at 20°) to the B telescopes during period 3 (also at 20°). After correcting for the difference in solid angles, etc., we infer a monitor change of $(-3.9 \pm 1.7)\%$ from period 3 to period 6.

Using the measured difference of 9.2% between periods 2 and 7 as fixed points on the monitor's drift path as a function of set number, the possible drift paths were assumed to be simple curves, which were adjusted to fit the abovementioned five pieces of data. A linear drift gave an excellent fit, and was used to obtain the needed corrections for the hydrogen data. By considering how far a drift path might deviate from linearity and still fit the data, a monitoring error of $\pm 1\%$ was inferred. The correction to and error in the cross section are listed in Tables IV and V, respectively.

Because the amount of deuterium in the target varied with time, deuterium-full data could not be used to provide information about the monitor drift path. By comparing the target-empty data of periods 8 and 9 for all counters, and of periods 4 and 12 for the 50° counters only, one finds a slower drift for the deuterium periods

TABLE V. All non-negligible errors in the cross section. Entries are percentage errors. The numbers in parentheses are errors in deuterium measurements when they differ from those in the hydrogen measurement. Given are the errors due to nuclear absorption (1), monitor drift (2), background and random subtraction (3), solid angle (4), random anticoincidence and inefficiency of counter 1 (5,6), uncertainty in mean energy (7), misalignment of target and telescope (8,10), misalignment of counter 2 (9), second-order angular effects (11), variation in energy threshold with angle (12), a partially full deuterium target (tgt), and counting statistics (13).

Angle	1 (abs)	2 (mon)	3 (sub)	4 (Ω)	5, 6 (ctr 1)	7 (δE)	8, 10 ($\delta\theta$)	9 (ctr 2)	11 (2nd)	12 (thr)	(tgt)	13 (stat)
A-15	0.9	1.0(4.0)	0.4(0.5)	0.8	0.3	0.2	0.6	0.0	0.1	0.5	(4.5)	0.9(1.1)
B-25	0.9	1.0(4.0)	0.5(0.7)	0.8	0.3	0.5	0.8	0.4	0.1	0.6	(4.5)	0.8(1.0)
C-40	0.9	1.0(4.0)	0.6(0.9)	0.8	0.3	0.3	0.8	0.8	0.2	0.8	(4.5)	1.0(1.4)
A-10	0.9	1.0(4.0)	0.5(0.6)	0.8	0.3	0.2	0.8	0.0	0.2	0.5	(4.3)	0.8(0.9)
B-20	0.9	1.0(4.0)	0.5(0.6)	0.8	0.3	0.3	0.8	0.4	0.1	0.6	(4.3)	0.7(0.8)
C-50	0.9	1.0(4.0)	1.1(1.0)	0.8	0.3	0.2	0.5	0.8	0.1	0.8	(4.3)	1.7(1.9)
A-20	0.9	1.0	0.4	0.8	0.3	0.3	0.8	0.0	0.1	0.5		0.8
B-30	0.9	1.0	0.4	0.8	0.3	0.5	0.9	0.4	0.2	0.6		0.8
C-45	0.9	1.0	0.5	0.8	0.3	0.2	0.6	0.8	0.1	0.8		1.0

than for the hydrogen periods. However, errors are sufficiently large so as to allow the same drift as for hydrogen periods, or no drift at all. For the corrections, we assume that the drift path was midway between, and use the extremes to obtain errors. The correction factors for periods 10 and 11 are 1.08 and 1.10, respectively. The relative error between periods 10 and 11 is $\pm 2\%$ and the absolute error between the hydrogen data and deuterium data is $\pm 3.5\%$.

It should be stressed that the monitor error does not affect the relative cross section of angles within the same data period, nor does it affect the polarization parameter.

3. Other Corrections and Errors

We have already discussed (1) absorber corrections and (2) monitor drift. Other corrections and errors that were considered include; (3) errors in the background and random subtraction procedure, (4) solid-angle corrections, with errors, (5) loss of good events through \bar{I} random anticoincidences, (6) inefficiency of anticoincidence counter \bar{I} , (7) uncertainty in the mean energy of the neutron beam, (8) misalignment of the 345 telescopes, (9) losses due to finite size and misalignment of counter 2, (10) target alignment, (11) spread in energy and angles (second-order effects), (12) variation in the energy threshold with angle, and (13) counting statistics.

Corrections to the cross section, errors in the cross sections, and errors in the polarization parameter, are listed in Tables IV, V, and VI, respectively. Any item in the above list that does not appear in a given table was found to be negligible. A complete discussion of all corrections and errors can be found in Ref. 5.

The main error contributions of about 1% come from

TABLE VI. All non-negligible errors in the polarization parameter. Given are the errors due to background and random subtraction (3), random anticoincidence and inefficiency of counter 1 (5, 6), uncertainty in mean energy (7), misalignment of target and telescope (8,10), second-order angular effects (11), and counting statistics (13).

Angle	3 (sub)	5, 6 (ctr 1)	7 ($\delta\bar{E}$)	8, 10 ($\delta\theta$)	11 (2nd)	13 (stat)
Hydrogen						
10°	0.0015	0.0008	0.0011	0.0012	0.0010	0.0120
15°	0.0025	0.0008	0.0016	0.0008	0.0010	0.0106
20°	0.0029	0.0008	0.0022	0.0004	0.0010	0.0078
25°	0.0022	0.0008	0.0028	0.0002	0.0010	0.0094
30°	0.0025	0.0008	0.0026	0.0003	0.0010	0.0108
40°	0.0042	0.0008	0.0054	0.0021	0.0030	0.0122
45°	0.0048	0.0008	0.0068	0.0032	0.0030	0.0143
50°	0.0105	0.0008	0.0060	0.0041	0.0030	0.0253
Deuterium						
10°	0.0017	0.0008	0.0011	0.0012	0.0010	0.0133
15°	0.0022	0.0008	0.0016	0.0008	0.0010	0.0157
20°	0.0032	0.0008	0.0022	0.0004	0.0010	0.0116
25°	0.0064	0.0008	0.0028	0.0002	0.0010	0.0141
40°	0.0053	0.0008	0.0054	0.0021	0.0030	0.0195
50°	0.0095	0.0008	0.0060	0.0041	0.0030	0.0266

the absorber, monitor, solid angle, energy-threshold corrections, and the errors on counting statistics. At the large angles the misalignment of counter 2 and the uncertainties in the background and random subtraction become sizeable. The error on the deuterium cross section is dominated by the error on the monitor correction and that caused by the partially full target.

All errors on the polarization are small except for the error on counting statistics. The use of the SFM and pairs of equal-angle counters cause the cancellation of most first-order effects and their errors.

4. Deuterium Data

The "three-nucleon" aspect of the deuterium data is best displayed by considering the ratio of deuterium to hydrogen cross sections, and the difference between the deuterium and hydrogen polarizations. In this way, some of the previously discussed errors cancel.

TABLE VII. Cross section and polarization for free n - p scattering. Listed are nominal laboratory scattering angle θ , the mean c.m. scattering angle $\theta_{c.m.}$, the c.m. relative differential cross section σ_{np} (arbitrarily normalized to 1.0 at 158.1°), and the polarization parameter P_{np} . In addition to the error listed for P_{np} , there is a systematic error of $\pm 10\%$, due to beam-polarization uncertainty, which will move all points together.

θ	$\theta_{c.m.}$	σ_{np}	P_{np}
10°	158.1°	1.000 \pm 0.021	-0.071 \pm 0.012
15°	148.1°	0.836 \pm 0.017	-0.117 \pm 0.011
20°	137.8°	0.701 \pm 0.015	-0.125 \pm 0.009
25°	127.4°	0.578 \pm 0.013	-0.125 \pm 0.010
30°	117.1°	0.461 \pm 0.010	-0.111 \pm 0.011
40°	96.3°	0.320 \pm 0.008	-0.075 \pm 0.014
45°	86.6°	0.292 \pm 0.007	0.029 \pm 0.017
50°	76.9°	0.273 \pm 0.008	0.132 \pm 0.028

However, there are two large sources of error affecting the deuterium data. One, the monitor drift, has been discussed already. The other was the fact that the deuterium target was not full. In fact, the content was varying with time, in a manner that could only roughly be determined. The correction factors to the cross section are 1.28 \pm 0.06 and 1.07 \pm 0.05 for data periods 10 and 11, respectively. Note that these large errors effect only the cross section, not the polarization. Both were due to technical difficulties, and were in no way intrinsic to the experimental approach.

C. Results

1. Cross Section

Free n - p cross section values are listed in Table VII. The error listed is the quadratic sum of the errors listed in Table V.

The ratio of the n - p cross section in deuterium to the free n - p cross section is given in Table VIII. Again, errors in Table V that do not cancel were combined quadratically. Two errors are listed: the relative errors within a data period, and the absolute errors.

TABLE VIII. Ratio of the cross section for the reaction $n+d \rightarrow p+2n$ to the cross section for free $n-p$ scattering, as measured (R_M), and as calculated by the impulse approximation (R_c). Two errors to R_M are given: $\delta R_M(R)$, the relative error within data period ($15^\circ, 25^\circ, 40^\circ$) or ($10^\circ, 20^\circ, 50^\circ$), and $\delta R_M(A)$, the absolute error.

Proton lab angle	R_M	$\delta R_M(R)$	$\delta R_M(A)$	R_c
15°	0.648	± 0.013	± 0.043	0.763
25°	0.660	± 0.015	± 0.044	0.759
40°	0.630	± 0.018	± 0.044	...
10°	0.665	± 0.014	± 0.044	0.738
20°	0.675	± 0.014	± 0.044	0.791
50°	0.597	± 0.021	± 0.043	...

2. Neutron-Beam Polarization

The measured asymmetries from the deuterium at 10° , 15° , 20° , and 25° , used to determine the neutron-beam polarization, are listed in Table IX. Also listed are the asymmetry parameters for the charge-symmetric reaction $p+d \rightarrow n+2p$, measured by Spalding *et al.*¹⁰ at 211 MeV, but here "shifted" to 199 MeV, using the energy dependence of the phase-shift solution (Y-IV) $_{np}$ of Breit and collaborators.¹¹ Their ratio is the neutron-beam polarization. Values for the four angles were averaged, yielding a beam polarization of 0.733 ± 0.075 . The error includes the relative errors on the data points, a 5% error in the normalization of Spalding's data, and 1% error due to the uncertainty in interpolating Spalding's data to 199 MeV.

3. Polarization Parameter

Free $n-p$ polarization parameter values are listed in Table VII. The error listed is the quadratic sum of the errors listed in Table VI. In addition, there is a systematic error of 10%, because of beam-polarization uncertainty, which will move all points together.

The difference between the polarization parameter for free $n-p$ scattering and $n-p$ scattering in deuterium is given in Table X. Again, errors in Table VI that do not

TABLE IX. Calculation of neutron-beam polarization. Listed are the measured asymmetry in the reaction $n+d \rightarrow p+(n+n)$ with the proton detected, ϵ ; the asymmetry in the reaction $p+d \rightarrow n+(p+p)$ with the neutron detected, from the data of Spalding, corrected to an energy of 199 MeV, P_{pn} ; and the beam polarization P_B , which is the ratio ϵ to P_{pn} , corrected for the energy dependence of the precession angle of the neutrons and for the finite size of the apparatus ($\cos\phi$).

Lab angle	ϵ	P_{pn}	P_B
10°	0.068 ± 0.009	0.095 ± 0.019	0.751 ± 0.181
15°	0.081 ± 0.011	0.122 ± 0.016	0.681 ± 0.126
20°	0.087 ± 0.008	0.107 ± 0.017	0.837 ± 0.153
25°	0.103 ± 0.010	0.147 ± 0.016	0.715 ± 0.120

¹¹ G. Breit, Rev. Mod. Phys. **39**, 560 (1967); and private communication.

TABLE X. Polarization parameter for the reaction $n+d \rightarrow p+2n$, P_{np}^D versus two-nucleon c.m. scattering angle $\theta_{c.m.}$. Also listed is the difference $P_{np} - P_{np}^D$ between the free and bound polarization parameters as measured, ΔP_M , and as calculated by the impulse approximation, ΔP_c .

$\theta_{c.m.}$	P_{np}^D	ΔP_M	ΔP_c
158.1	-0.098 ± 0.014	0.027 ± 0.018	0.013
148.1	-0.114 ± 0.016	-0.003 ± 0.019	0.010
137.8	-0.127 ± 0.012	-0.003 ± 0.015	0.006
127.4	-0.144 ± 0.016	$+0.019 \pm 0.018$	0.002
96.3	-0.040 ± 0.021	-0.035 ± 0.026	...
76.9	$+0.061 \pm 0.029$	0.071 ± 0.041	...

cancel were combined quadratically to obtain the listed error. Errors due to beam-polarization uncertainty are 10% of the difference, and are quite negligible.

V. DISCUSSION

A. Review of $n-p$ Differential Cross-Section Measurement near 200 MeV

The relative differential cross section has been measured over the entire angular range 0° – 180° by Kazarinov and Simonov.¹² The neutron beam used was created by deuteron stripping; it had a mean energy of 200 MeV and a spread of 40 MeV full width at half-maximum. Recoil protons were detected at scattering angles $67\frac{1}{2}^\circ < \theta_{c.m.} < 180^\circ$; scattered neutrons were detected at smaller c.m. angles. Accuracy was typically $\pm 3\%$ when protons were detected, and $\pm 15\%$ when neutrons were detected. The results, taken from the compilation of Wilson,¹³ are listed in Table XI. They have been normalized to an $n-p$ total cross-section measurement of Kazarinov and Simonov.¹² They disagree with the older, nominally less accurate measurements of Guernsey, Mott, and Nelson¹⁴ by more than the claimed combined errors, at angles near 100° .

TABLE XI. $n-p$ differential cross-section measurements of Kazarinov and Simonov (Ref. 12) as given in the compilation of Wilson (Ref. 13).

$\theta_{c.m.}$ (deg)	σ (mb/sr)	$\theta_{c.m.}$ (deg)	σ (mb/sr)
6.25	9.5 ± 2.5	117.5	3.51 ± 0.24
10.5	8.3 ± 0.8	129.6	3.85 ± 0.16
21.3	4.7 ± 0.7	139.3	4.63 ± 0.16
31.5	4.1 ± 0.5	148.5	5.79 ± 0.12
41.7	3.0 ± 0.4	159	7.02 ± 0.13
62.7	2.4 ± 0.4	163	7.78 ± 0.24
67.3	2.16 ± 0.16	165	9.22 ± 0.26
77.3	1.91 ± 0.07	169.5	10.33 ± 0.23
87	1.87 ± 0.08	173.75	11.29 ± 0.24
97	2.20 ± 0.08	180	11.4 ± 0.4
109.3	2.79 ± 0.16		

¹² Yu. M. Kazarinov and Yu. N. Simonov, Zh. Eksperim. i Teor. Phys. **43**, 35 (1962) [English transl.: Soviet Phys.—JETP **16**, 24 (1963)].

¹³ Richard Wilson, *The Nucleon-Nucleon Interaction* (Interscience Publishers, Inc., New York, 1963).

¹⁴ G. Guernsey, G. Mott, and B. Nelson, Phys. Rev. **88**, 15 (1952).

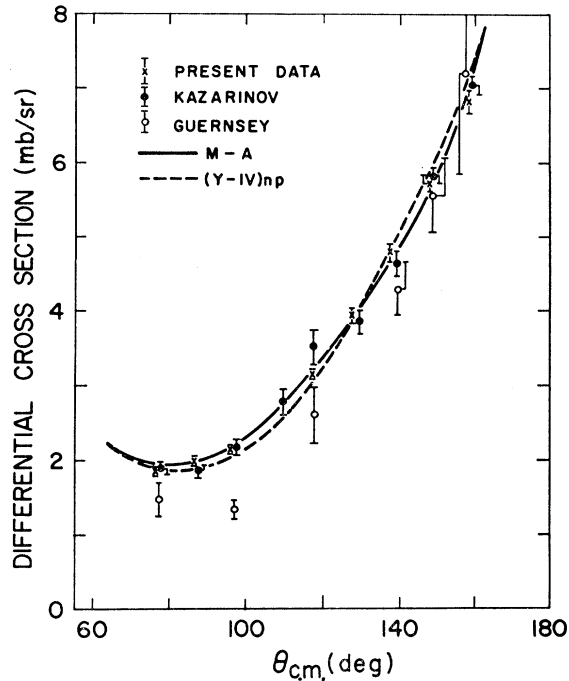


FIG. 5. n - p cross-section measurements of Kazarinov and Simonov (Ref. 12), Guernsey *et al.* (Ref. 14), and the present work. Also shown are the phase shift solutions $(Y-IV)_{np}$ of Breit (Ref. 11) and of MacGregor and Arndt (Ref. 15). Our data have been normalized to agree with the phase-shift solutions at 158° .

The results of Kazarinov and Simonov (KS),¹² of Guernsey,¹⁴ and of the present authors are plotted in Fig. 5. It is seen that our results and those of KS agree well, and both disagree with the measurements of Guernsey *et al.* It is recommended that the results of Guernsey *et al.* not be used in any analysis of n - p data, but that both the present results and those of KS be used.

Also shown in Fig. 5 are phase-shift solutions of Breit and collaborators¹¹ $(Y-IV)_{np}$ and of MacGregor and Arndt (MA).¹⁵ The curves are in good agreement with our data, and with KS's, but disagree with the data of Guernsey *et al.* The phase-shift searches have used KS's data, but not our data, as input. (It should be noted that our data have been normalized to agree with the phase-shift solutions at 158° .)

B. n - p Polarization Measurements

Tinlot and Warner¹⁶ measured $P(\theta)$ in quasifree p - n scattering from deuterium, at 217 MeV, from 40° to 120° c.m. Both scattered proton and recoiling neutron were detected. A CD_2 -C subtraction was employed. Using the energy dependence suggested by the Yale phase-shift analyses,¹¹ we have "shifted" Tinlot and Warner's measurements to 199 MeV and plotted them

¹⁵ M. H. MacGregor and R. A. Arndt, Phys. Rev. **139**, B362 (1965).

¹⁶ J. H. Tinlot and R. E. Warner, Phys. Rev. **124**, 890 (1961).

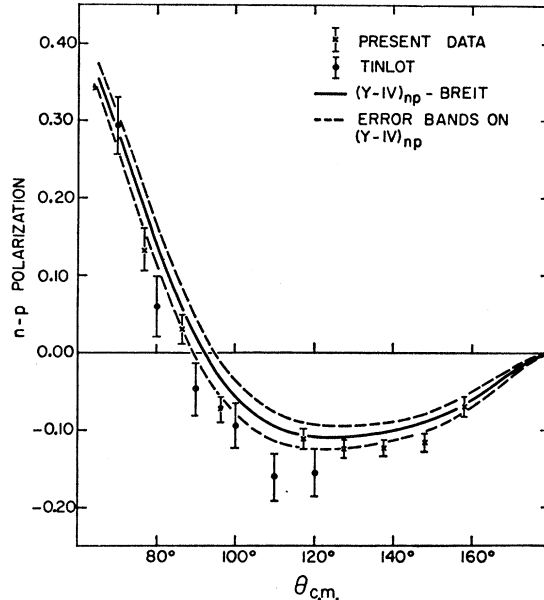


FIG. 6. n - p polarization measurements of Tinlot and Warner (Ref. 16), and the present work. The results of Tinlot have been shifted to 199 MeV (see text). Not included in the plotted errors are a systematic error of ± 0.04 in Tinlot's measurements due to the use of quasifree scattering, and a systematic error of $\pm 10\%$ in our measurements due to the beam-polarization uncertainty. Also shown is the phase-shift solution $(Y-IV)_{np}$, with error bands (Ref. 11).

in Fig. 6. For angles from 40° to 90° , a "correction" relating these measurements to the free n - p polarizations has been applied.¹⁷ Systematic errors in this correction due to theoretical uncertainties, perhaps as large as ± 0.04 , have not been included in the plotted errors. Our measurements are also shown in Fig. 6. The 10% systematic error due to the beam-polarization uncertainty is not included in the plotted errors. The agreement with Tinlot and Warner's points is satisfactory.

It is recommended that in any analysis of n - p data the results of Tinlot and Warner not be used at angles greater than 70° . Our measurements have significantly smaller random errors, and a systematic error ($\pm 10\%$, due to beam-polarization uncertainty) that is smaller and more reliably determined than the systematic error from using quasifree p - n scattering (estimated at ± 0.04).

Phase-shift solution $(Y-IV)_{np}$, with error bands,¹¹ is also shown in Fig. 6. Agreement with our data is fair.

C. n - p Scattering in Deuterium

An impulse-approximation calculation of the reaction $n+d \rightarrow p+2n$, with only the proton being detected, has been performed.¹ The s -wave final-state interaction of the two neutrons is allowed for by a square-well potential; other final-state interactions are ignored.

¹⁷ P. F. M. Koehler, E. H. Thorndike, and A. Cromer, Phys. Rev. **134**, B1030 (1964).

The ratio of the free $n-p$ cross section, as calculated and as measured, is listed in Table VIII. The effect of the energy threshold of this experiment was included in the calculation. Note that the measured ratio, typically 0.65 ± 0.04 , is significantly smaller than the calculated ratio, typically 0.76. Note also that the measured ratio is quite angle-independent (except at the largest lab angle, 50°), as is seen by the constancy of R_M within a data period, where the smaller error, $\delta R_M(R)$, applies.

The difference between polarization parameters for

free $n-p$ scattering and for the reaction $n+d \rightarrow p+2n$, as measured and as calculated, are listed in Table X. The measured difference is small, consistent with the calculated difference, but also consistent with zero.

ACKNOWLEDGMENTS

We gratefully acknowledge the participation of Dr. N. W. Reay in the early stages of this experiment. We thank Professor Breit for sending us extensive results of his phase-shift analyses.

Forward π^-p Charge-Exchange Scattering between 561 and 2106 MeV/c*†‡

WINTHROP S. RISK

Princeton University, Princeton, New Jersey

(Received 11 August 1967)

Final results are presented from a spark-chamber experiment performed at the Princeton-Pennsylvania Accelerator to measure the differential cross section near 0° for the reaction $\pi^-p \rightarrow \pi^0n$. The data are extrapolated to 0° and the results of the extrapolation are compared with the results of other experiments and with dispersion relation predictions. The values of the forward-scattering amplitude for the fifteen values of incident π^- momentum at which measurements were made are as follows: (p (MeV/c), $(d\sigma/d\Omega)_0^\circ$ (mb/sr)): (561, 3.28), (636, 2.95), (687, 3.38), (750, 2.48), (802, 1.33), (930, 2.42), (1005, 3.15), (1030, 3.43), (1077, 1.70), (1134, 1.04), (1434, 0.31), (1579, 0.56), (1711, 0.73), (1914, 0.87), (2106, 0.56). The combined statistical and systematic uncertainties in these values is about $\pm 9\%$. A description of the apparatus, a discussion of the methods of analysis, and a discussion of the errors contributing to the uncertainties in the above results are included in the text.

I. INTRODUCTION

THIS experiment was performed at the Princeton-Pennsylvania Accelerator (P.P.A.) in the fall of 1964 at which time the available measurements of the π^-p charge-exchange forward amplitude $[d\sigma/d\Omega(0^\circ)]$ were those below 550 MeV/c¹ and those of Saclay² in the interval 900–2000 MeV/c. The measurements below 550 MeV/c offered convincing experimental proof of the pion-nucleon dispersion relations developed by Goldberger *et al.*³ These relations, involving no assumptions about the dynamics of the pion-nucleon interaction, express $d\sigma/d\Omega(0^\circ)$ in terms of integrals over the elastic total cross sections $\sigma(\pi^\pm p \rightarrow \pi^\pm p)$. The Saclay mea-

surements showed generally good agreement with the dispersion relations, but were systematically high around 1500 MeV/c.

There are now available measurements of the total angular distributions for $\pi^-p \rightarrow \pi^0n$ ⁴ in the energy region covered by this experiment and a number of recent measurements of $\sigma(\pi^\pm p \rightarrow \pi^\pm p)$.⁵ Dispersion calculations of $d\sigma/d\Omega(0^\circ)$ have been published beginning with the work of Cronin,⁶ but the most detailed calculations and comparisons with the experimental data have been done by Höhler *et al.*⁷ Reference 7 also gives a fairly complete summary of the experimental and theoretical work to date.

As these additional results become available, it was

* Work supported by the U. S. Office of Naval Research under Contract No. AT(30-1)3406.

† Based in part on a thesis submitted in partial fulfillment of the requirements for the degree of Doctor of Philosophy in Physics, Princeton University.

‡ This work made use of computer facilities supported in part by National Science Foundation Grant No. NSF-GP 579.

¹ V. G. Zinov and S. M. Korenchenko, Zh. Eksperim. i Teor. Fiz. **36**, 618 (1959) [English transl.: Soviet Phys.—JETP **9**, 429 (1959)]; J. C. Caris, R. W. Kenney, V. Perez-Mendez, V. A. Perkins, Phys. Rev. **121**, 893 (1961).

² P. Borgeaud, C. Bruneton, Y. Ducros, P. Falk-Vairant, O. Guisan, J. Movchet, P. Sonderegger, A. Stirling, M. Yvert, A. Tran Ha, and S. D. Warshaw, Phys. Letters **10**, 134 (1964).

³ M. L. Goldberger, H. Miyazawa, R. Oehme, Phys. Rev. **99**, 986 (1955); M. L. Goldberger, *ibid.* **99**, 979 (1955).

⁴ L. Guerriero, Proc. Roy. Soc. (London) **A289**, 471 (1966); C. B. Chiu *et al.*, Phys. Rev. **156**, 1415 (1967). The author wishes to thank Professor R. E. Lanou of Brown University for providing more recent results than those of Guerriero.

⁵ W. Galbraith, E. W. Jenkins, T. F. Kycia, B. A. Leontic, R. H. Phillips, A. L. Read, and R. Rubenstein, Phys. Rev. **138**, B913 (1965); T. J. Devlin, J. Solomon, and G. Bertsch, Phys. Rev. Letters **14**, 1031 (1965); B. Amblard, P. Borgeaud, Y. Dueros, P. Falk-Vairant, O. Guisan, W. Laskar, P. Sonderegger, A. Stirling, M. Yvert, A. Tran Ha, and S. D. Warshaw, Phys. Letters **10**, 138 (1964).

⁶ J. W. Cronin, Phys. Rev. **118**, 824 (1960).

⁷ G. Höhler, J. Baacke, and R. Strauss, Phys. Letters **21**, 223 (1966); G. Höhler, J. Baacke, J. Giesecke, and N. Novko, Proc. Roy. Soc. (London) **A289**, 500 (1966).